Mechanical Constraints on the Development of the Zagros Folded Belt (Fars)

F. Mouthereau · O. Lacombe · J. Tensi · N. Bellahsen · S. Kargar · K. Amrouch

Abstract. We synthesize available structural, seismotectonics and microtectonics studies, mechanical modelling of the topography as well as stratigraphic constraints on the timing of Plio-Pleistocene folding and Zagros basin evolution in order to examine which mechanical behaviour would explain the development of the Zagros Folded Belt at both local and regional scale.

At the local scale we focus on the mechanism of cover folding and internal deformation of cover rocks. At the regional scale we focus on crustal rheology that led to the observed regional topography. Recent mechanical constraints derived from a critical wedge modelling of the regional topography together with available structural studies and seismotectonic studies confirm that the basement is necessarily involved in the deformation. Additionally, crustal rheology should involve a sufficiently strong lower crust to maintain the topography.

Stratigraphic data on the basin scale suggests that the deformation in the Zagros Folded Belt initiated by inversion of the inherited N-S and NW-SE-trending marginal structures in the early Miocene. At 5–3 Ma, the intraplate stresses have increased sufficiently in response to ongoing convergence to exceed the brittle strength of the pre-fractured basement and then to produce the initiation of the Zagros uplift. This event occurred simultaneously with the rapid development of cover folding until the Bakhtyari conglomerates were deposited unconformably on these structures as the fold growth decreased. The Hormuz salts at the base of the pile allowed the upper sedimentary cover to be decoupled from the basement but there is no evidence of independent development through time. This is confirmed by the kinematical consistency of the Mio-Pliocene small-scale faulting in the cover and seismogenic faulting reflecting the internal deformation of basement and cover, despite the occurrence of the thick Hormuz salt layer. Buckling of the cover rocks, rather than thin-skinned propagation of the Zagros Folded Belt, is proposed to be a more reliable mechanism to account for stratigraphic data, field observations, structural studies, microtectonic data and mechanical modelling.

We finally conclude that the overall thick-skinned deformation that followed the initial margin inversion was probably coeval with cover folding (buckling). The way basement and cover deform is thus remarkably different; the basement is pre-fractured so it shortens preferentially by faulting. In contrast, the folding (buckling) of the sedimentary cover developed with the assistance of plastic-viscous processes.

1 Introduction

The Zagros Mountains form a broad orogenic domain in Iran, approximately 2000 km long and 100–200 km wide in front of the Turkish-Iranian plateau (Fig. 1). The mountain range results from the accommodation of the convergence between the rifted continental margin of the Arabian plate and the Iranian continental block, which followed the closure of the neo-Tethys ocean during the Tertiary [Stocklin, 1968; Berberian and King, 1981; Koop and Stoneley, 1982]. The present-day convergence between Arabia and Eurasia is ~3 cm/yr and about 7 mm/yr is currently accommodated across the Zagros collision belt [Vernant et al., 2004].

The collision suture zone is outlined by the Main Zagros Thrust that separates the Sanandaj-Sirjan domain to the North from the Imbricate Zone and the Zagros Folded Belt (ZFB) to the South. The Sanandaj-Sirjan belt is a broad tectono-metamorphic belt which represents the former active margin of the Iranian microplate (Fig. 2). To the South, the Imbricate Zone and the Zagros Folded Belt, separated by the High Zagros Fault, form a large folded domain within the rifted Arabian continental margin. The Imbricate Zone is mainly composed of folded Mesozoic strata (Fig. 2) but locally along the Main Zagros Thrust, ophiolitic rocks, remnants of the obducted ocean or one of its derivatives (e.g., back-arc or fore-arc oceans) are preserved [Stoneley, 1990; Ziegler, 2001].

In this paper we focus on the Central Fars province of the ZFB (Fig. 2). This area is located between the Dezful-Izeh domain to the northwest recently documented by several studies [e.g. Blanc et al., 2003; Sherkati and Letouzey, 2004], and the Bandar-Abbas province at the southeastern extremity of the Fars area investigated by Molinaro et al. [2005]. The Central Fars is a 200 km-wide arcuate folded belt, which results from folding of a thick pile of sedimentary rocks up to 12 km in thickness [Stocklin, 1968] including Paleozoic, Meso-Cenozoic strata and Neogene syno-

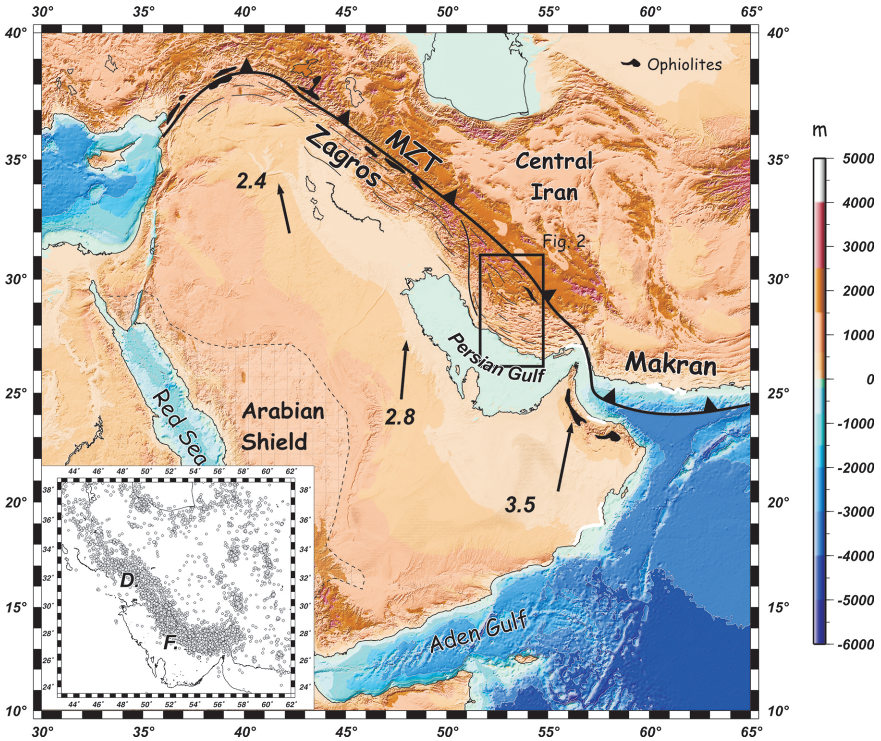

Fig. 1. Geodynamic framework of the Zagros Folded Belt. *Black arrows* show the present-day convergence between the Arabian plate and stable Eurasia deduced from current global plate motion Nuvel 1A [De Mets et al., 1994]. It predicts a present-day convergence of ~3±0.5 cm/yr oriented N-S on average at the front of the Zagros Mountains. The *grey rectangle* indicates the study area of the Fars province. The *inset* shows the distribution of earthquakes (2.4 <mb <7.4) in the Zagros collision belt with focal depths lower than 35 km issued from ISC and CMT catalogs (1965-2003). Many of the earthquakes in the Zagros correspond to events occurring in the basement. Inset : D. for Dezful and F. for Fars areas

rogenic deposits (Fig. 3). The deformation in the Fars area is characterized by periodic folding with axial lengths sometimes greater than 200 km (Fig. 2).

The exceptional geomorphic expression of folding is linked to the presence, within the folded pile, of the competent carbonates of the Asmari Formation, Oligo-Miocene in age, which is one of the main oil reservoirs in the Zagros. The Fars domain of the ZFB is limited to the West by a main structural, topographic and paleogeographic boundary: the Kazerun fault [Motiei, 1993; Sepher and Cosgrove, 2005] (Fig 1). It is a major N-S trending active right-lateral strike-slip fault inherited from the Late Proterozoic fault system of the Pan-African basement [Talbot and Alavi, 1996].

Cover folding is generally thought to be explained by the occurrence of a thick (up to 2 km) incompetent layer of salt at the base of the cover within the Eo-Cambrian series of the Hormuz Formation (Fig. 3). This basal décollement allows decoupling of the sedimentary cover from the underlying Precambrian series and crystalline basement. In addition to this main décollement, second-order shallower detachment levels lying in the sedimentary pile present in other parts of the Zagros Folded Belt [Sherkati and Letouzey, 2004; Molinaro et al., 2005a] may also have been potentially active during folding in our study area. One of the major issues that should be addressed is the mechanisms of folding that produce such a large folded belt. Indeed, no consensus exists so far on whether folding is simply thrust-related folding accommodating shortening in a brittle cover [McQuarrie, 2004; Sherkati and Letouzey, 2004; Molinaro et al., 2005] or a consequence of buckling of the sedimentary rocks [e.g. Schmalholz et al., 2002; Mouthereau et al., 2006]. In the first type of models, it is the accommodation of deformation associated with cover thrusting which produces folding. In contrast, for the second type of models, folding is caused by mechanical instabilities within the competent cover overlying an incompetent layer. In this case, if faulting occurs it is not the cause but rather the consequence of folding. It is obvious that the mechanical implications of both models in terms of rocks rheology and mechanics of the folded belt are very different.

A second controversy concerns the recent uplift of the ZFB. If the timing of the Zagros uplift is relatively well constrained by a regional unconformity, two different mechanisms have been proposed to explain it: crustal shortening [Mouthereau et al., 2006] or thermal anomaly [Molinaro et al., 2005b]. Whatever the uplift mechanism, seismotectonic studies [Berberian, 1995; Talebian and Jackson, 2004; Tatar et al., 2004] together with subsurface data and cross-section balancing [Blanc et al., 2003; Sherkati and Letouzey, 2004] have suggested that basement-involved shortening may be essential to explain the anatomy of the Zagros folded belt.

Our objective in this paper is to examine which type of mechanical behaviour would better explain particular features observed in the Zagros folded belt at both local and regional scales. On the local scale we

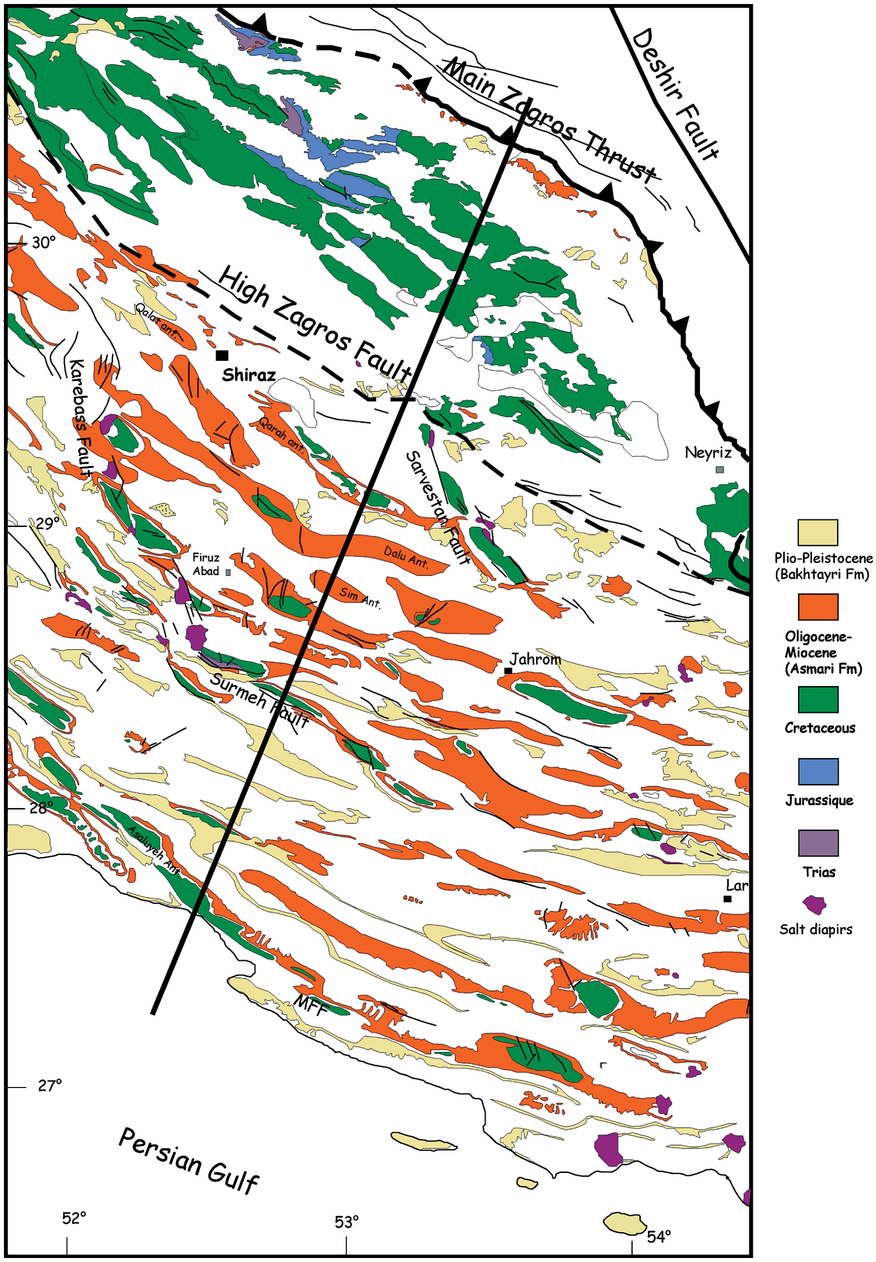

Fig. 2. Simplified geological map of the Fars province of the Zagros Folded Belt (based on the National Iranian Oil Company [1977]. The Imbricate Zone to the North of the High Zagros Fault is clearly distinguished from the Zagros Folded Belt to the South by the lack of Oligo-Miocene deposits. The *heavy black solid line* displays the location of geological section of Fig. 4

focus on the mechanics of cover folding and how internal deformation is accommodated in cover rocks. On the regional scale we focus on crustal rheology. To this aim, we synthesize available structural studies to constrain the first-order geometry of folds and the location of major basement thrust faults. These data are used to build a crustal-scale section of the Central Fars. Recent modelling of critical wedges [Mouthereau et al., 2006] as well as recently published seismotectonics and microtectonics studies [Lacombe et al., 2006] including recent results on calcite twinning [Amrouch et al., 2005] are combined together with new field observations to constrain the mechanics and the timing of deformation that prevailed in both the sedimentary cover and the basement.

2 From Rifting to Collision of the Arabian Margin: Stratigraphy of the Zagros Basin

We first introduce the Zagros collision belt in the framework of the opening then the closure of the Neo-Tethys. To this purpose, we summarize hereinafter the

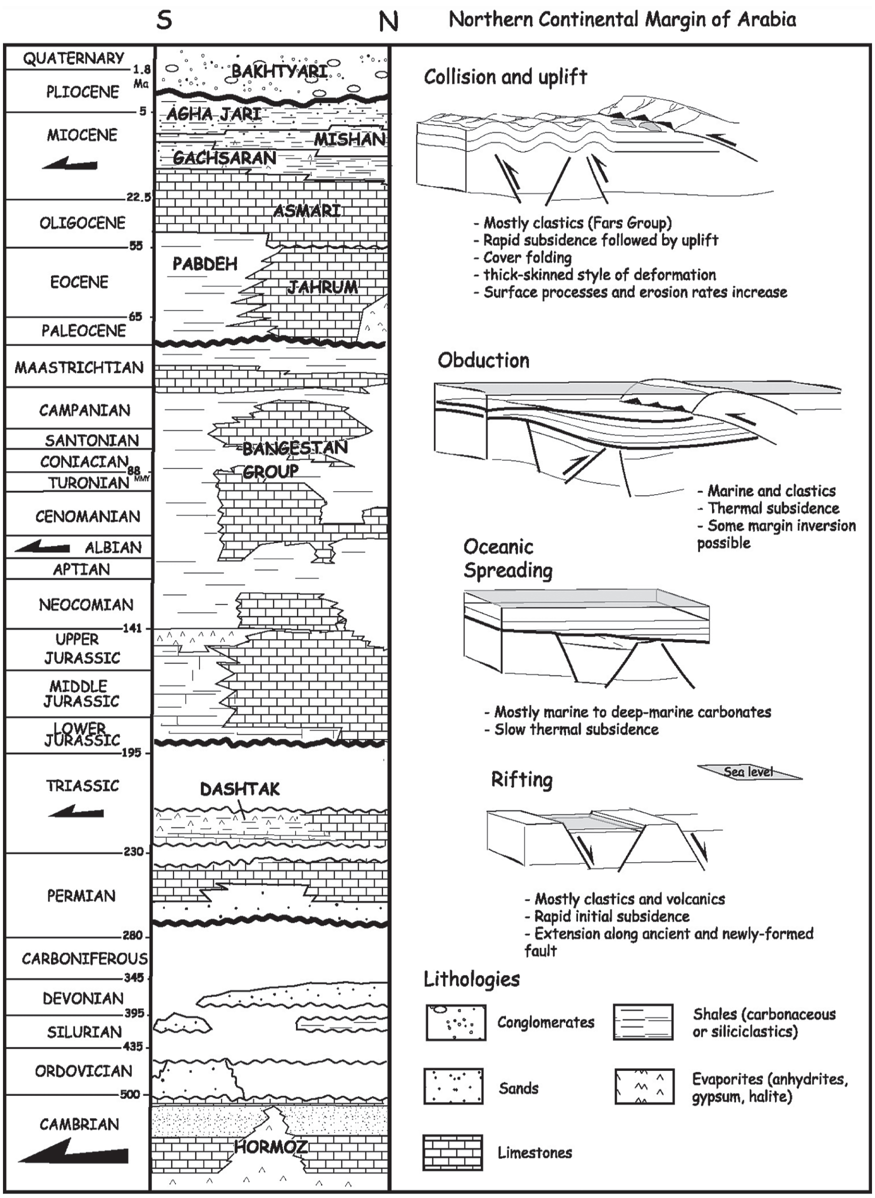

Fig. 3. Simplified chronostratigraphic chart and lithologies encountered in the Central Fars folded belt after [Motiei, 1993]. *Sketches on the right* show the main tectonic events reported on the Arabian continental margin. The basal décollement (*black arrow*) of the folded cover lies within the Eo-Cambrian salts of the Hormuz formation. *Other black arrows* refer to second-order detachment levels encountered in other parts of the Zagros belt

main tectonic events recorded on the Arabian continental margin in the ZFB since the Paleozoic.

Following the Hercynian orogeny, by the end of the Paleozoic, the Arabian lithosphere was stretched (Fig. 3). This episode is recorded in the Zagros basin by a main unconformity at the base of mid-Permian carbonates together with the occurrence of Permian clastics and volcanics in the High Zagros [Koop and Stoneley, 1982]. Extension affected the Zagros crystalline basement and produced a series of NW-trending grabens parallel to the current orientation of the Zagros Belt [Sepher and Cosgrove, 2004]. This fracture pattern is superimposed on an older Precambrian set of fractures in the basement trending N-S oblique to the Zagros main trend [Talbot and Alavi, 1996]. The Neo-Tethyan rifting initiated at the Trias-Jurassic boundary. A major unconformity at the base of the Jurassic series records this transition. Since this time, the Arabian continental passive margin developed with a different sedimentological pattern than in Central Iran which has drifted away. During the Upper Cretaceous (Campanian), isopachs reveal the presence of a narrow trough located to the south of the present position of the MZT [Koop and Stoneley, 1982]. From the Upper Cretaceous-Paleocene limit until the Eocene the conditions of deposition changed dramatically and subsidence clearly increased to the NW, especially in the Dezful-Izeh domain of the ZFB [Koop and Stoneley, 1982; Sherkati and Letouzey, 2004]. The early Neogene period is characterized by deposition of the carbonates of the Asmari Formation on the Arabian continental margin and of the Qom Formation on the Iranian plateau. Biostratigraphic constraints yield an age ranging from upper Oligocene to lower Miocene for both formations (Chattian-Aquitanian boundary) [Schuster and Wielandt, 1999]. Post-Asmari clastics, known as the Fars Group including the Gashsaran, Mishan and Agha Jari Formations (Early Miocene to Pliocene), have a total thickness of up to 3000 m in the Fars area [Koop and Stoneley, 1982] indicating a rapid tectonically-controlled subsidence. This Group forms a progradational synorogenic sequence in the subsident Zagros foreland basin fed by the products of the erosion of the hinterland that was thickening and uplifting. This stage is considered by several authors as being controlled by the final closure of the Neo-tethyan ocean [Elmore and Farrand, 1981; McQuarrie et al., 2003; Agard et al., 2005] leading to the development of the Zagros orogeny.

The presence of local angular unconformities and disconformities within the folded belt indicates that the Arabian continental margin was probably deforming earlier than generally thought. For instance, Hessami et al. [2001] suggested that folding in the ZFB started at the end of the Eocene and then propagated in-sequence southwards in thin-skinned style. Sherkati and Letouzey [2004] suggested from isopach maps in the NW Zagros that compressive deformation might have been initiated in the upper Eocene-Oligocene times.

Ahmadhadi et al. [this issue] also report an early Miocene reactivation and inversion of NWtrending inherited Tethyan normal faults in the Zagros foreland. This emphasizes that the Arabian continental margin underwent compression, inversion and basement-involved shortening during the early stage of the collision.

The last period of sedimentation is characterized by the deposition of alluvial conglomerates of the Bakhtyari Formation throughout the ZFB whose base is dated at 3 Ma in the Northeastern part of the ZFB [Homke et al., 2004]. As continental deposits, the Bakhtyari Formation is probably diachronous both along-strike and across-strike of the Zagros Folded Belt. Regarding the Fars Group whose first-order sedimentary characteristics support ongoing foreland basin evolution, the unconformable deposition of conglomerates on top of previously folded strata suggests that the main phase of shortening in the ZFB occurred before 3 Ma. It is worth noting that such changes in the type of deposition suggest modifications in the efficiency of erosion driven by global cooling well documented at that time [e.g., Molnar and England, 1990] or/and by uplift related to Zagros collision.

3 Mechanical Modelling of the Topography: a Critical Wedge Approach

3.1 Thin-Skinned versus Thick-Skinned Model: a Short Review

The presence of a thick and weak salt-bearing formation (i.e., the Hormuz Formation) has led for years to interpret the style of cover folding as resulting from fault-related folding that developed in a thin-skinned style, in agreement with the critical wedge model described by Davis and Engelder [1985]. These authors applied the theory of Coulomb wedges to thin-skinned frictional wedges overlying a ductile decollement. Such salt-based wedges are characterized by low topographic slopes and the absence of clear vergence of folding. The lack of clear fold vergence (Fig. 4) and the observations of low topographic slopes < 0.5° (Fig. 5) seem to support this model. Sand-box experiments involving silicone putty as analogous to viscous properties of salt décollement provided additional constraints on the way the spatial distribution of salt controls the shape of the Zagros Folded Belt and the sequence of deformation [Jackson et al., 1990; Weijermars et al., 1993; Costa and Vendeville, 2002; Bahroudi and Koyi, 2003]. Ongoing cover folding is further supported today by GPS surveys across the ZFB [Walpersdorf et al., in press] and is consistent with quaternary folding at the Mountain Front evidenced through dated tilted marine terraces [Oveisi et al., this issue].

On the other hand, seismotectonic studies over the last 20 years have provided several lines of evidence that the Precambrian basement is shortening and thickening [Jackson, 1980; Berberian and King, 1981; Ni and Barazangi, 1986; Berberian, 1995]. Active basement-involved shortening was confirmed by new accurate estimates of the depths of earthquakes [Talebian and Jackson, 2004; Tatar et al., 2004]. Furthermore, balanced cross-sections have shown that different topographic elevations of the base of the Paleozoic and Mesozoic Formations required basement involvement [Blanc et al., 2003; Sherkati and Letouzey, 2004; Molinaro et al., 2005a].

It consequently appears that the Zagros Folded Belt is actively deforming by superimposed thin-skinned and thick-skinned styles. In order to examine the relative involvement of both thin-skinned and thick-skinned deformation to explain the origin of the present topographic slope, a critical wedge modelling has been recently carried out [Mouthereau et al., 2006]. The main results are summarized hereafter. This work aimed at comparing the observed topographic slopes with that derived from modelling of 1) a shallow brittle wedge of sedimentary cover detached above a salt

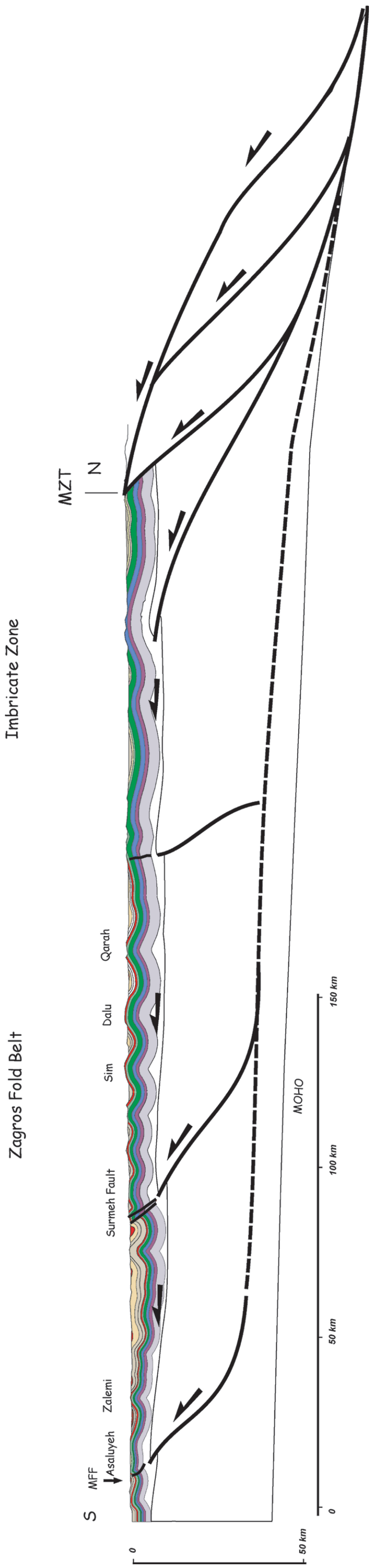

◀ **Fig. 4.** Crustal-scale geological section across the Zagros Folded Belt in the Central Fars. This section attempts at accounting for 1) faulting in the basement especially along the MFF and the Surmeh Fault, 2) decoupling between cover folding and seismogenic basement-involved deformation, 3) lack of evidence for fault-related folds features in the cover as well as 4) the variations in sedimentary rock thicknesses. Note the decrease of fold wavelengths from the Imbricate Zone toward the Surmeh Fault

décollement; 2) a thick brittle wedge of upper crystalline basement decoupled above a ductile lower crust.

3.2 Mechanical Modelling of the ZFB as a Thin-Skinned Critical Wedge

In this model the strength of sedimentary rocks is limited by a Coulomb failure criterion. The convenience of this simple model is that it can be directly compared with structural constraints in existing cross-sections, which assumes fault-related fold geometries, or with other models of salt-based fold-thrust belts. When the state of stress within the wedge attains a critical value, a critical taper is achieved, which is defined by the sum of the dip of its base β (taken positive toward the hinterland) and the dip α of its upper topographic slope (taken positive toward the foreland). The equation that provides the relationship between the wedge taper angle $\alpha+\beta$ and the basal shear stress τ_b and internal friction angle ϕ in the thrust wedge (after [Davis and Engelder], 1985]) is given by

$$\alpha + \beta = \frac{\beta + \left(\dfrac{\tau_b}{\rho_{sed}\, gH}\right)}{1 + (1-\lambda)\left(\dfrac{2}{[1/\sin(\phi)]-1}\right)} \tag{1}$$

where α is the topographic slope of the wedge (positive toward the foreland), β is the slope of the basement (positive toward the hinterland), λ is the pore fluid pressure ratio within the wedge, τ_b is the yield stress of the salt, ϕ is the angle of internal friction (between 30° and 40°), ρ_{sed} is the average volumetric mass of the wedge and H is the thickness of the wedge.

The forces in the salt resisting the advancement of the wedge are believed to be accommodated by simple shear. To constrain the value of the décollement dip β (basement top) we assumed that the top of the basement is parallel to the Moho discontinuity. The dip of the Moho ranges between 0.6° and 1° based on seismological constraints [Hatzfeld et al., 2003] and inversion of gravity data [Snyder and Barazangi, 1986], respectively. Taking into account the slope of the basement

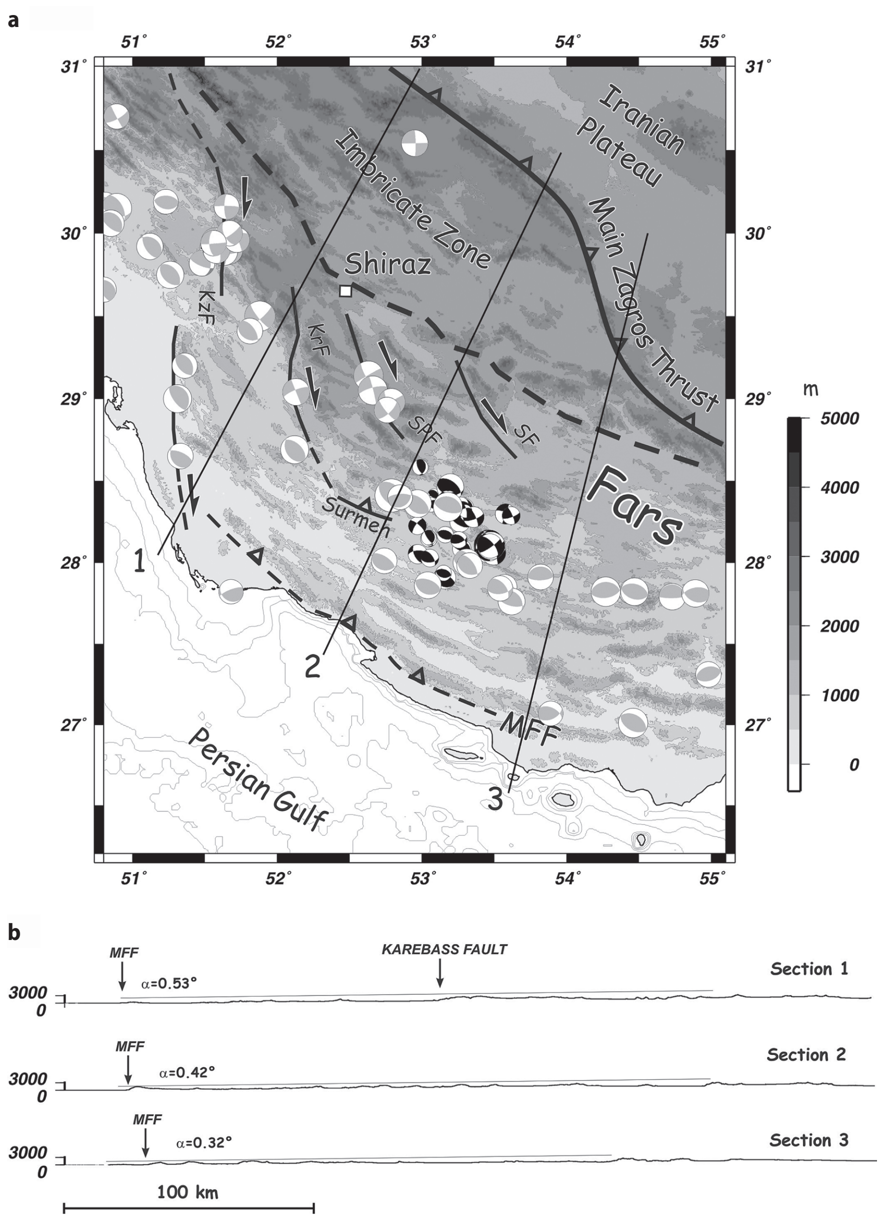

Fig. 5. a Topography (SRTM data) and main structural features and **b** topography derived from SRTM data and topographic slopes estimated along sections 1, 2 and 3 located in a. The folded sedimentary cover is decoupled from the basement above the Hormuz Salt Formation. The present-day and long-term deformation within the basement is attested along the MFF and the Surmeh Fault in agreement with the position of the main basement faults presented by several works [Berberian, 1995; Talebian and Jackson, 2004]. Focal mechanisms reveal that the basement is deforming and thickening along distributed faults probably inherited from Permo-Triassic rifting. Fault plane solutions (4.6 <Mw < 6.7) [from Talebian and Jackson, 2004] are shown with focal spheres in light gray. Focal mechanisms of small earthquakes (1.7 < ML < 4.1) determined from local network [Tatar et al., 2004] are shown with black focal spheres

derived from restored sections [McQuarrie, 2004] we finally adopted a value of 0.5°.

The "steepest" topography or the highest topographic slope (~ -0.33°) is obtained for the highest basal shear stress (443 kPa) and the lowest angle of internal friction (30°) (Fig. 6a). The lowest topographic slope (~ -0.39°) is obtained for a lower basal shear stress (11 kPa) and a higher internal friction (40°). It is clear, despite relatively important variations between each model, that the predicted topography is essentially flat. This result reveals that the sedimentary cover and the underlying salts are both remarkably thick in the Zagros. As a result, the ratio $\tau_b / \rho_{sed} g H$ in Eqn (1) is very small of the order of 10^{-3}. This illustrates that when a thick layer of salt (relatively to its overburden) forms the basal décollement it is generally too weak and cannot support the growth of significant topography. We concluded that the observed topographic slopes across the ZFB can not be reproduced by a salt-based wedge model.

3.3 Mechanical Modelling of the ZFB as a Thick-Skinned Critical Wedge

An alternative is to consider that the Zagros topography results from the thickening of the brittle basement, in agreement with current seismogenic activity,

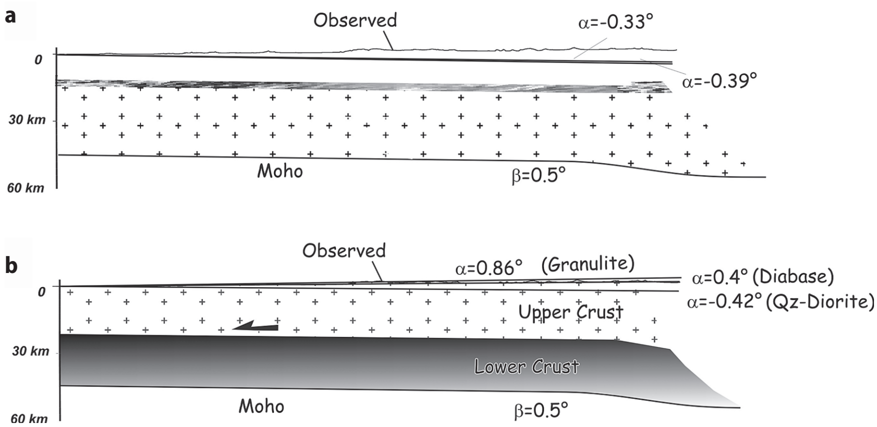

Fig. 6. **a** Topographic slopes modelled by a thin-skinned wedge of brittle materials overlying a ductile décollement. **b** Topographic slopes modelled by a thick-skinned critical wedge of brittle upper crust sliding over a ductile (non-Newtonian) lower crust for which different rock types are used [after Mouthereau et al., 2006]

that is decoupled above a viscous lower crust. Studies of receiver functions revealed a crustal thickness of 45 km and a ~25 km-thick lower crust [Hatzfeld et al., 2003]. This is consistent with the deepest small earthquakes, observed at 18 km by Tatar et al. [2004] and the depth distribution of major and moderate earthquakes shown by Maggi et al. [2000]. At such depths, temperature-activated ductile deformation in the crust predominated and dislocation creep of minerals occurs. The deviatoric yielding stresses in the lower ductile crust thus follow a power law that is dependent on temperature and strain rates. In order to cover a wide range of viscosities, different rock types such as quartzite for weak lower crust and mafic composition like diabase, quartz-diorite or granulite for stronger lower crust were tested. A cold crustal geothermal gradient of 10–15°C/km was assumed in agreement with temperatures required, at Moho depth, to produce continental subduction.

Assuming a quartz-diorite rheology, a negative value of -0.42° (taper angle of 0.08°) is obtained for α (Fig. 6b). In this case, similarly with the salt-based wedge hypothesis, the lower crust is too weak and cannot maintain the observed topography. In contrast, when stronger rheologies (diabase or granulite) are used, positive topographic slopes of 0.4° and 0.86°, respectively (equivalent to tapers of 0.9° and 1.36°), are obtained in agreement with the observed topography.

In contrast to the thin-skinned hypothesis, we demonstrate that the shortening of the basement above a viscous lower crust is able to reproduce the observed topography. We note that rock composition in the lower crust should necessarily comprise sufficiently strong (mafic) materials. We conclude that although thin-skinned deformation obviously occurs, basement-involved shortening is responsible for the present-day topography.

After having demonstrated that basement-involved shortening is the only viable mechanism to account for the current regional topography, we now examine both geological observations and constraints from the topography, which support long-lived basement tectonics.

4 Evidence for Long-Lived Faulting in the Basement

4.1 Topographic Steps Related to Basement Faulting

Despite the apparent continuity of structures, morphology and surface geology, two locally important topographic steps and structural features are recognized: the Mountain Front Fault (MFF) and the Surmeh Fault, 100 km apart (Fig. 5). Using wavelengths analysis of the topography, these faults clearly affect the overall topography over distance comprised between 40 km and 100 km [Mouthereau et al., 2006].

In the following, we have used the nomenclature defined by Berberian [1995] for major faults. The MFF [Berberian, 1995] is also called the Mountain Front Flexure by Falcon [1961] or the Zagros Frontal Fault by Sepher and Cosgrove [2004]. These latter authors named the Surmeh Fault, the Mountain Front Fault.

The Mountain Front Fault is not directly observable in the field. Its topographic expression is however clearly depicted along the coastline of the Persian Gulf as it is formed by a girdle of en-échelon folds over more than 200 km (Fig. 7). Topographic profiles show a clear topographic step, across the MFF, which is outlined by the uplift of the local base level up to 700 m (e.g., Asaluyeh anticline, profile 1 of Fig. 7). The second topographic offset is about 500 m and occurs across the faulted Surmeh Anticline, one of the few folds of the ZFB where Paleozoic strata are exposed.

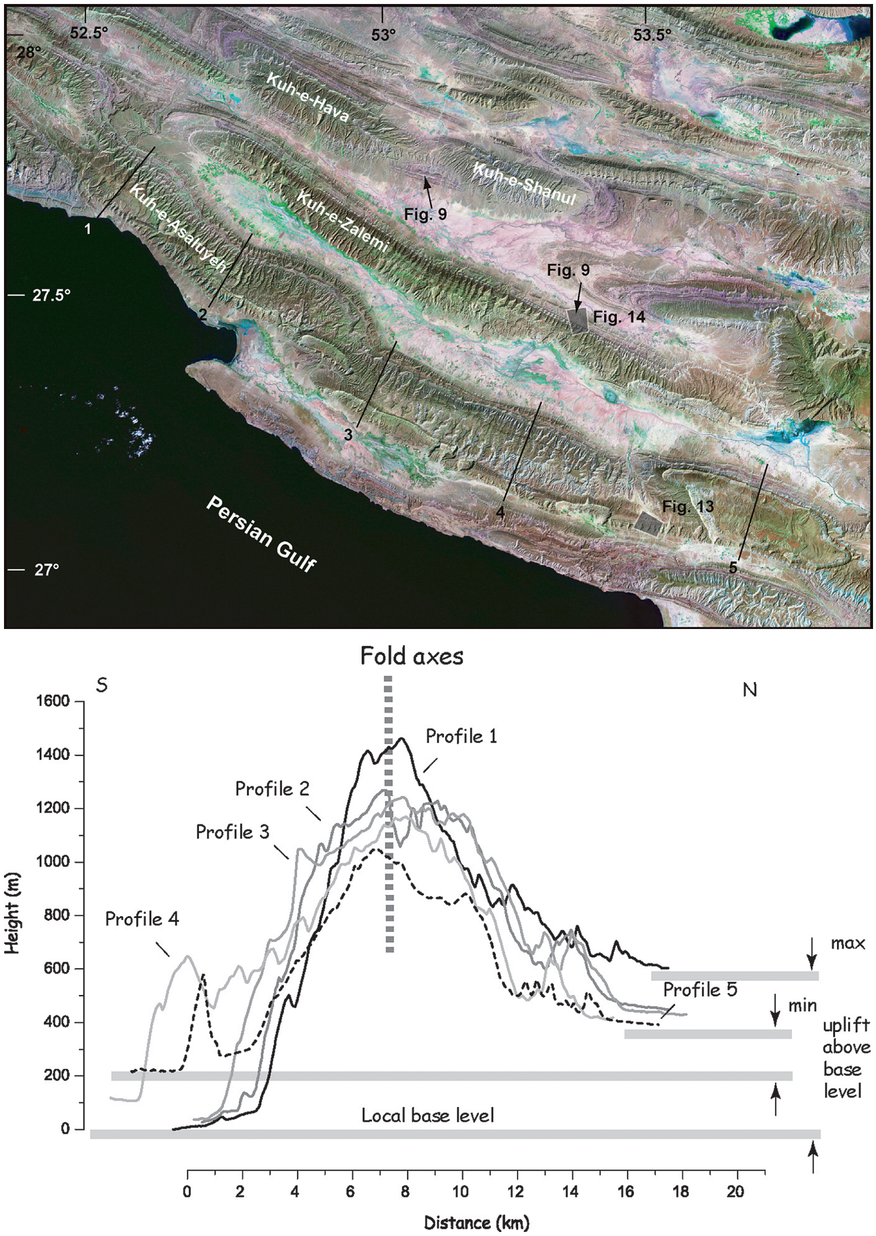

Fig. 7. *Top*: Landsat 7 (TM) image of the southern Central Fars province. Large-scale folds bordering the Persian Gulf and related to the Mountain Front Fault (including the Asaluyeh anticline) are well depicted. Topographic profiles across these folds are shown *below*. All topographic profiles are plotted with a common reference frame, i.e. their fold axes

4.2 Current State of Stress in the Basement

Most of the thrust earthquakes in the Zagros Folded Belt occur between the coast of the Persian Gulf and the Surmeh thrust zone (Fig. 5). In this context, the present-day activity of the Mountain Front and Surmeh faults has been demonstrated by extensive seismotectonic analyses by Berberian [1995]. For instance, recent destructive earthquakes like the Ghir (1972, M_S=6.9) and the Lar (1966, M_S=6.2) earthquakes [Berberian, 1995] aligned along the trace of the Surmeh topographic step and form the Surmeh-Ghir thrust zone. The Surmeh-Ghir thrust zone is connected with the Karebass Fault, a major right-lateral transverse fault rooted into the basement (Fig. 5). For the MFF, Berberian [1995] has suggested that the location of the Asaluyeh anticline coincides exactly with the trace of a major seismic trend along which large-to-moderate earthquakes occur on buried, high-angle basement reverse fault segments.

The present-day stress regimes in the Fars have been recently derived from available focal mechanisms of earthquakes [Lacombe et al., 2006]. The inversion process applied to a set of moderate earthquakes [Talebian and Jackson, 2004] and microearthquakes [Tatar et al., 2004] led to subhorizontal σ1 axis trending N209°(±15) and N206°(±5) respectively. Noticeably, the value of the Φ=(σ2-σ3/σ1-σ3) ratio in both cases is low (<0.3) suggesting σ2/σ3 stress permutations. Such a regime and the absence of clear structural relationships between strike-slip/reverse mechanisms and major strike-slip/reverse (Surmeh-Ghir) faults shows that basement deformation depicted by microearthquakes at the local scale is rather distributed and occurred under both reverse faults and right-lateral strike-slip faults.

The computed N020–030° compressional trend is in good agreement with the pattern and kinematics of active faults in the western Fars [Baker et al., 1993; Berberian, 1995]. It is also consistent with current geodetic (cover) and seismic (basement) strain shortening axes which are coaxial and oriented N010° on average [Masson et al., 2005].

4.3 Long-Lived Basement Thrusting: Constraints from Middle Miocene Basin Geometry

The Mishan Fm is a well-defined transgressive interval within the Fars Group outlined by the deposition of limestones, silts and bioclastics throughout the Zagros foreland basin. In the Zagros basin, the isopachs of the Mishan Formation provide further constraints on the paleo-topography at the time of deposition, i.e. in Middle to Upper Miocene times (Fig. 8).

The base of the Mishan Fm varies from about 600 m depth at the latitude of Firuz Abad and attains about 900 m southward. A large depocenter developed in the Coastal Fars area between the MFF and the Surmeh Fault and a large portion of the northern Fars domain, roughly limited by the Sabz-Pushan and the Karebass strike-slip faults, is uplifted. Since the subsidence is more pronounced in the depression located in the hangingwall of the Karebass-Surmeh fault, we infer the possibility that basement-involved deformation locally affected the Zagros basin during the Middle Miocene. On average, the isopachs south of Shiraz suggest that the overall subsidence in the basin was controlled regionally by plate flexure and locally by basement thrust loading.

At the southern border of the Zagros basin, in the forelimb of the Asaluyeh anticline, the Gashsaran Formation and the base of the Mishan Formation are missing above the Asmari Limestones [Mouthereau et al., 2006]. This field observation is correlated with isopach maps of the Neogene strata showing at larger scale that the Mishan are continuously thinning toward the MFF. Furthermore, it is also across this anticline that the morphological step is the largest suggesting long-lived basement thrusting along the

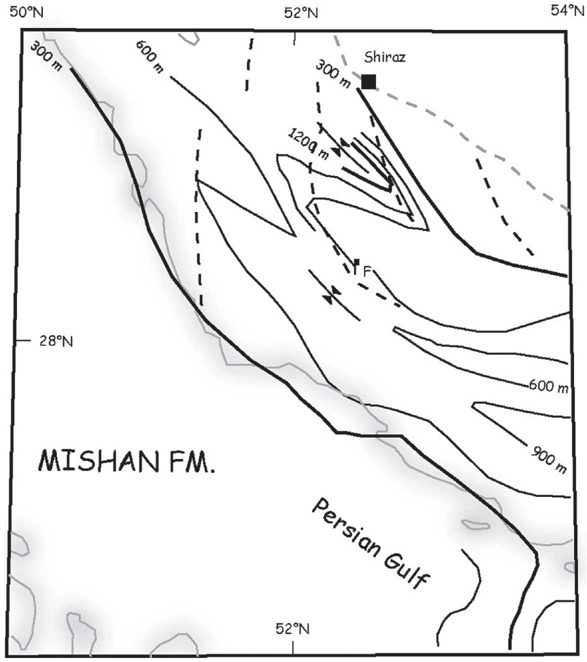

Fig. 8. Isopach maps of the Mishan Formation. Equidistance is 300 m. Main depocenters are shown by *converging arrows*. F: Firuz Abad. *Black dashed lines* correspond to major active transverse structures, e.g., the *one passing* close to Firuz Abad depicts the position of the Karebass-Surmeh Fault

MFF (Fig. 7). We suggest that this stratigraphic hiatus was locally uplifted above sea-level during the upper Miocene. This might be a consequence of basement involvement along the buried MFF, but alternative possibilities such as forebulge uplift or local amplification due to cover folding should be also envisaged.

Whatever the style of deformation, this would suggest that the deformation had already reached the current location of the Mountain Front Fault by Middle-Miocene times.

In summary, it appears that basement-involved deformation occurs mainly by faulting and initiated at least in the Middle Miocene during an early phase of margin inversion.

5 The Main Phase of Cover Folding: Evidence from Unconformities within the Agha Jari and Bakhtyari Formations

We have seen that basement-involved shortening along the Surmeh-Karebass faults segment or the MFF initiated in the Middle Miocene prior to the main phase of cover folding.

On the other hand, GPS studies [Walpersdorf et al., in press] and dated tilted marine terraces [Oveisi et al., this issue] indicate that cover folding is currently active with a significant accommodation of shortening across the MFF. According to field observations, the existence of intraformational unconformities within the Agha Jari Formation has been recognized for years in the Dezful or Lorestan areas [e.g. Hessami et al., 2001; Homke et al., 2004]. This places strong constraints on the timing of the initiation of folding in the cover and the rate at which these folds developed. However, no evidence of such unconformities has been described in the Central Fars so far.

During our field investigations in the Central Fars, numerous unconformities or disconformities have been reported within the Agha Jari Fm. However, many of them are not progressive unconformities but rather correspond to unconformities of limited extension, typically of several tens of meters, probably not related to tectonics (Fig. 9). On the other hand, when synclinal sections were available, several progressive intraformational unconformities were observed that are clearly correlated with fold growth.

The first example of folds that clearly display progressive intraformational unconformities within the Upper Agha Jari Formation is found to the North of Shiraz in the vicinity of the Qalat anticline (Fig. 10). The total thickness of the Agha Jari Formation and Bakhtyari Formation reaches 700 m and form cliffs on both limbs of the Qalat fold. The older strata, i.e. the Upper Agha Jari Fm, show progressive unconformities revealing coeval fold activity to the north. The Bakhtyari strata do not display progressive unconformities but are rather onlapping the underlying folded strata of the Upper Agha Jari Fm toward the crest of the fold.

Another observation of progressive unconformities is found in association with the growth of the Karbasi anticline about 200 km southeast (Fig. 11). Despite the large distance between both folds several similarities are found. For instance, the cliff formed by the Bakhtyari conglomerates displays no evidence of intraformational unconformity. In contrast, the lower and older strata belonging to the Agha Jari Fm show progressive unconformities that can be related to the development of the Karbasi anticline.

Though more observations and stratigraphic constraints are required to draw an accurate image of the sequence of folding, we suggest that the upper Agha Jari strata are synfolding whereas the overlying Bakhtyari conglomerates are mainly post-folding.

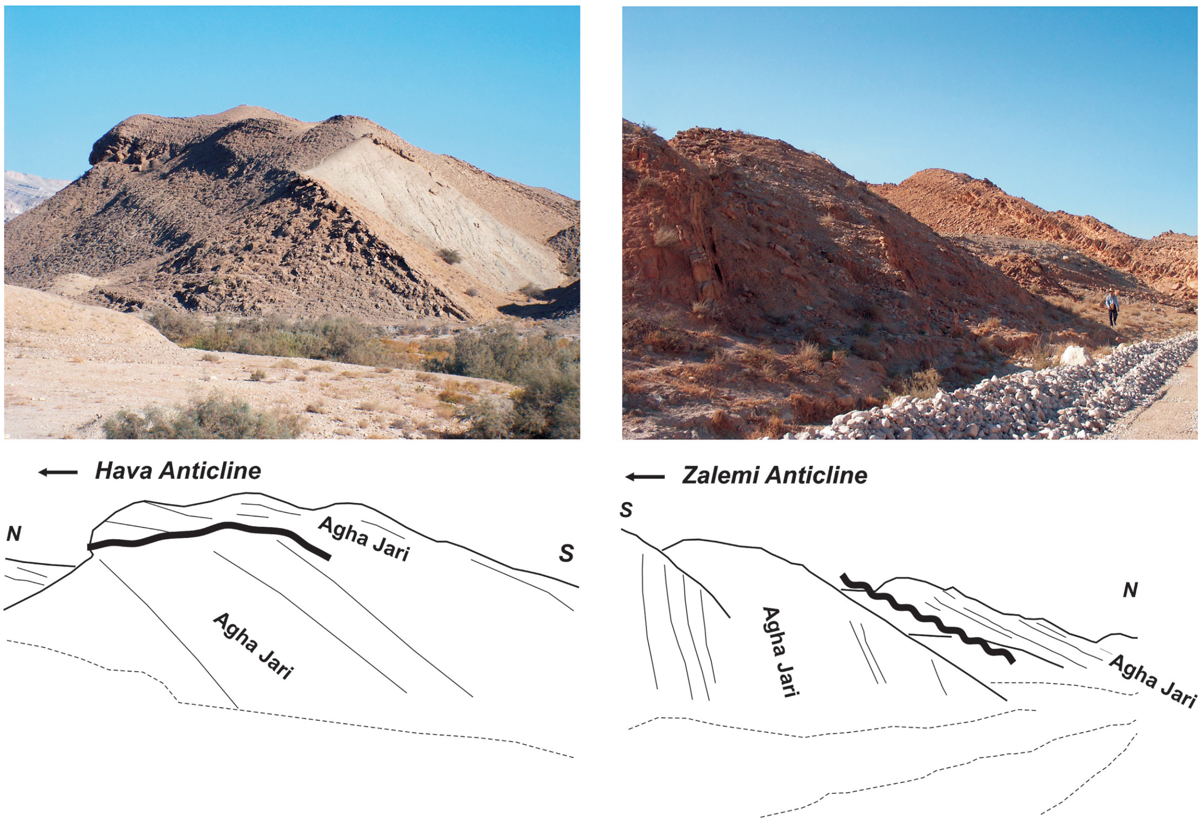

Fig. 9. Examples of intraformational unconformities within the Agha Jari Formation of two fold limbs located in the Southern Central Fars (see Fig. 7 for location). These unconformities are not progressive and of local extent. They are probably not related to fold activity but rather to sedimentary processes in the ancient alluvial plain

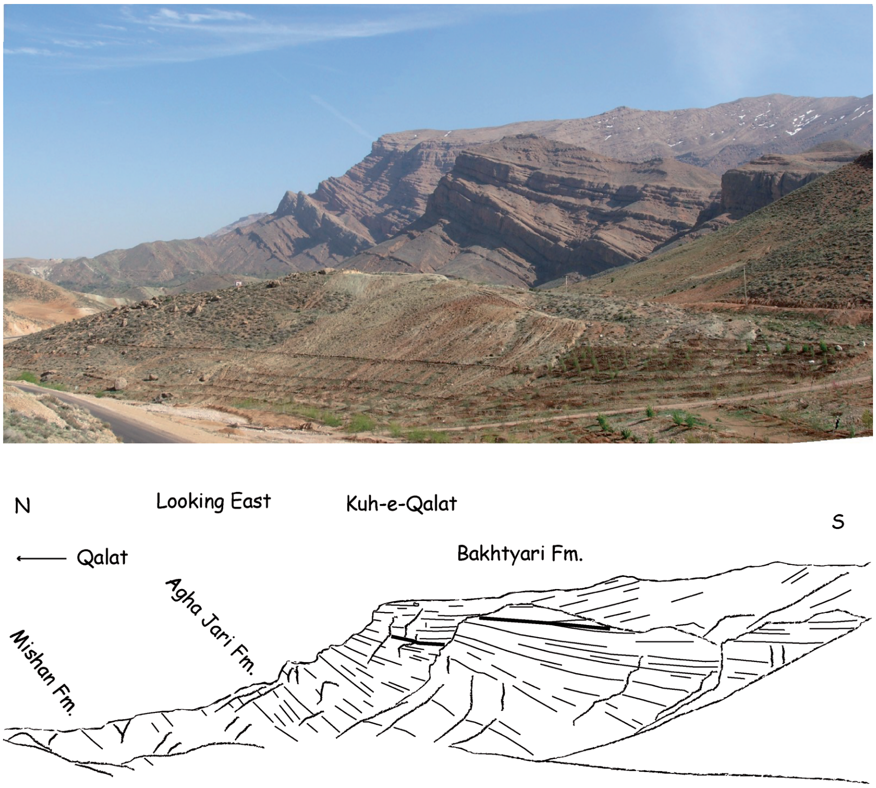

Fig. 10. Intraformational unconformities within the upper Agha Jari strata North of the Qalat anticline (see Fig. 2 for location). The upper alluvial conglomeratic beds of the Bakhtyari Fm onlap the older strata of the Agha Jari thus suggesting a slowing down of fold uplift relatively to sedimentation rates

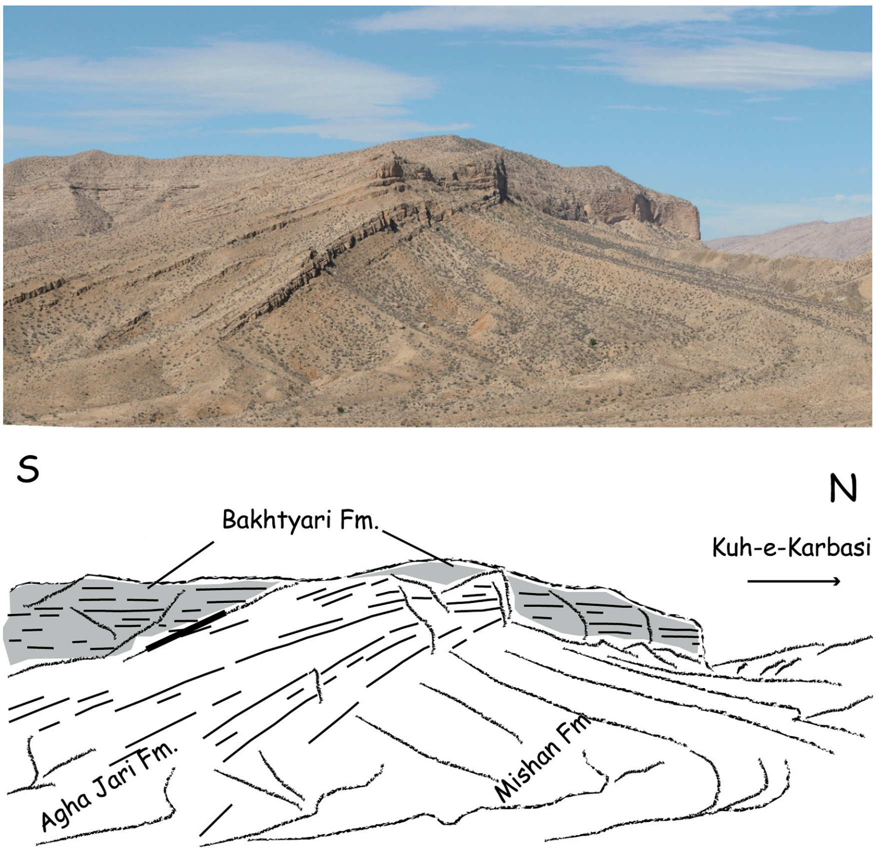

Fig. 11. Intraformational unconformities within the upper Agha Jari strata to the South of the Karbasi anticline (see Fig. 2 for location). The cliff shows the upper alluvial conglomeratic beds of the Bakhtyari Fm. They clearly onlap the older strata of the Agha Jari again suggesting a slowing down of fold uplift relatively to the sedimentation rates

The same chronology has been proposed in the Dezful area [e.g. Homke et al., 2004]. In the Coastal Fars, this inference is supported by the observation that the youngest conglomerates usually unconformably overlie folded strata. The duration of synfolding unconformities ca. 2–2.5 Ma. is approximated by the age of the top of the folded strata, i.e. Upper Agha Jari Fm, and the age of the base of the Bakhtyari Fm provided by Homke et al. [2004] in the Dezful-Izeh area.

This indicates that the folds growth was initially rapid in association with limb rotation. The lack of evidence for diachronous folding further suggests that folding rather occurred coevally across the strike of the belt. Moreover, the geometry (onlaps) of the Bakhtyari conglomerates with respect to underlying folded Agha Jari Formation reveals that the rate of fold uplift decreased with respect to the rate of deposition of the Bakhtyari conglomerates in the Zagros foreland. This provides constraints on the overall mechanism which produced rapid fold development coevally across the Zagros Folded Belt.

6 Long-Term Rheology of Folded Cover Rocks: Insights from Folding Geometry and Mesoscale to Microscale Tectonic Studies

Figure 4 shows a schematic 300-km-long cross-section of the Zagros Fold Belt including the Imbricate Zone. This section has been constructed using structural constraints from NIOC geological maps [National Iranian Oil Company, 1977], structural dips at surface, variations in layers thickness within the Meso-Cenozoic strata based on well data [Motiei, 1993]. The lack of faults at the surface except where active basement thrusts are reported (e.g. MFF, Surmeh, Karebass, Sabz-Pushan fault zone) makes dubious a systematic involvement of thrusting to explain folds in the sedimentary cover. We do not exclude however, when shortening increased and fold limbs rotated, that faulting occurred due to deformation in the fold hinges, but this is not supported by any field observations in our study area.

6.1 Distribution of Fold Wavelengths and Topographic Signature of Folding

Figure 12 shows the distribution of fold wavelengths for 149 folds measured between two successive synclines, in the Eastern and Western Fars areas. A monomodal distribution of the fold widths clearly appears on the graph showing a dominant wavelength of cover folding between 10 and 20 km representing 70% of the measured folds. One important parameter that mechanically controls the observed dominant wavelength of folding is the thickness of the deformed competent units. Despite some scatter, the Gaussian distribution of fold widths would suggest that a single main competent level is involved. It is worth noting that the presence of intermediate detachment layers described in the Dezful and Bandar-Abbas areas [Sherkati and Letouzey, 2004; Molinaro et al., 2005] is weakly supported by field observations in the Central Fars. Though probably not exhaustive, field observations carried out in the Central Fars only reported the possible involvement of intermediate detachments close to the MFF (Figure 13). Inversely, when well-known incompetent layers such as the Gashsaran Fm can be observed at the surface, they are not involved in the compressional deformation (Figure 14). If other potential detachment like the evaporitic Dashtak Fm (Trias) present only in the Coastal Fars accommodates folding it would lead to lower dominant wavelengths of folds, which are not observed. It thus comes that intermediate detachment layers are of second-order importance to explain the wavelength of folding. Indeed, they only affect the superficial folding style at a scale lower than the dominant wavelength of folding.

As a consequence this would not change our main conclusion that folding is mechanically explained to a first-order by one single detachment level.

A simple relation might exist between the depth to which crustal deformation occurs and the wavelength of its topographic expression; the thicker the deformed unit the larger the wavelengths of deformation. The analysis of wavelengths in the topography can be also qualitatively used as a proxy to distinguish different

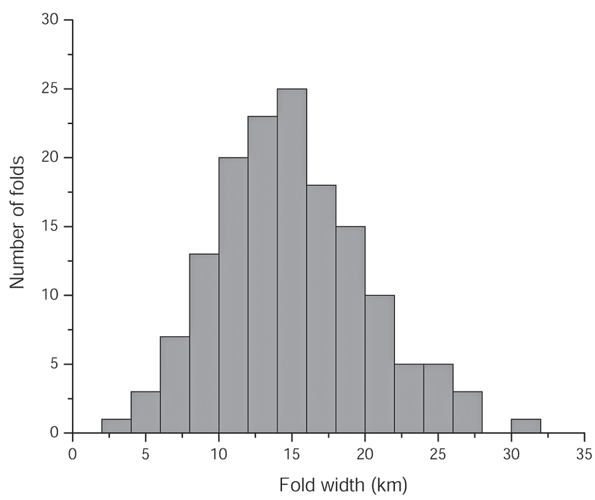

Fig. 12. Distribution of fold widths measured for 149 anticlines in the Fars (see text for explanation). Fold widths have been estimated as the distance between two adjacent synclines independently from the stratigraphy of the folded strata. 101 folds (70% of the measured folds) have wavelengths between 10 and 20 km

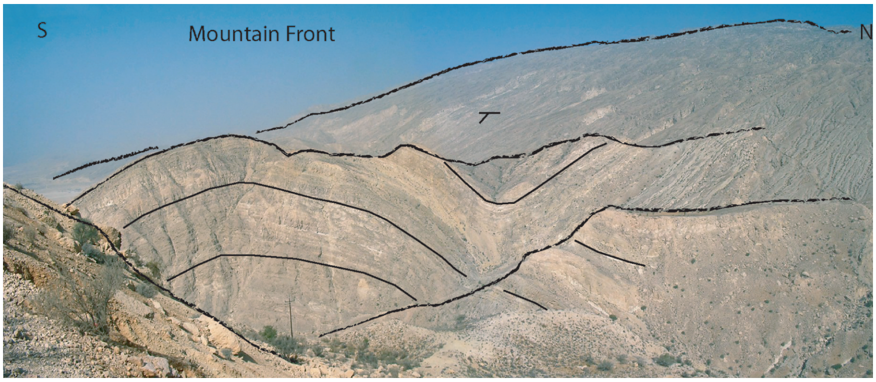

Fig. 13. Example of smaller scale folding in the southern limb of one of the larger scale folds in relation to the Mountain Front Fault (see location on Fig. 7). Such features are atypical in the Central Fars domain and mostly observed along the Mountain Front

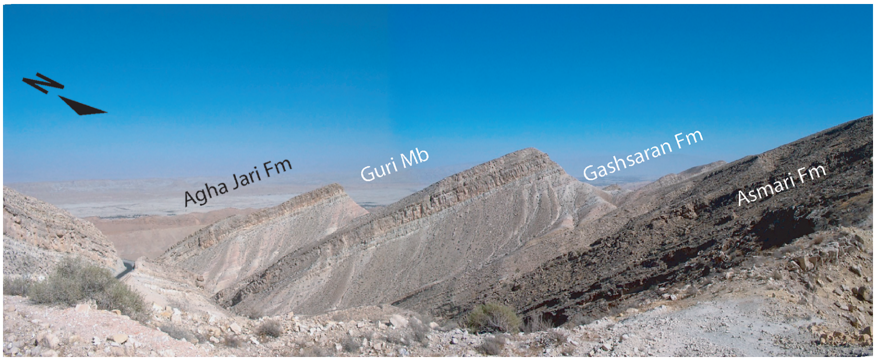

Fig. 14. Northern limb of the Zalemi anticline (see location on Fig. 7). Note the normal stratigraphic succession in the Fars Group (Mishan Fm is not visible on this photograph) above the Asmari carbonates. Like many other examples over the Central Fars, the incompetent layers of the Gashsaran Fm (mainly gypsum with marls) do not act as an intermediate detachment

levels of deformation [Mouthereau et al., 2006]. Figure 15 shows 2-D analysis of topographic wavelengths along the strike of the Fars folded belt along three topographic sections. High-pass and low-pass filters were applied to the 3' x 3' gridded SRTM topography.

For example, when wavelengths larger than 40 km, i.e. the maximum wavelength of cover folding (Fig. 15), are removed, the remaining topography of folds shows amplitude reaching 1000 m. These are found 1) close to major active basement fault zones, e.g., the sharp increase of the elevation near the Gulf corresponds to the position of the MFF (Sects 2 and 3), 500 to 1000 m are correlated with the position of active transpressive strike-slip faults such as Kazerun (KzF), Karebass (KrF), Sabz-Pushan (SPF) or Sarvestan (SF) faults; 2) for folds flanked by more deeply incised synclinal valleys or 3) for folds whose development is perturbed by the ascent of salt diapirs, especially in the southern-eastern part of the ZFB (Sect 3). Despite such local perturbations, the deformation associated with folding is remarkably homogeneous in amplitudes and wavelengths and is consequently not visible on the residual topography. This topographic pattern again suggests, in addition to the distribution of fold widths, that the mechanism of folding is primarily controlled by the thickness of the competent cover. Independently from mechanical assumptions, similar conclusions are also supported by balanced cross-sections [McQuarrie, 2004; Sherkati and Letouzey, 2004]. The quasi-sinusoidal shape of the short-wavelength component of the topography related to folding appears simply superimposed onto larger wavelengths, i.e. larger than 40 km, which reflects basement-involved thickening (Fig. 16).

6.2 Mechanical Behaviour of the Cover Sequence: Constraints from Mesoscale Faulting and Microscale Calcite Twinning

Field observation of folding has revealed that mesoscale faulting is often associated with shear calcite fibers in the few carbonaceous beds of the Fars Group or in the Asmari Formation and gypsum fibers in local evaporite facies from Gachsaran Formation and Agha Jari Formation. In addition, pervasive pressure solution accompanied faulting as evidenced by widespread stylolitization. Hydraulic breccia in some sites indicates that local high fluid pressures assisted faulting. Moreover, analysis of calcite twin strain (Fig. 17) has been carriedout for limestones of the Pabdeh-Gurpi, Asmari-Jahrom, Gachsaran and Mishan Formations [Dissez, 2004; Amrouch, 2005]. The twin shapes reveal that the deformation occurred at temperature lower than 150–200°C and that internal strain did not

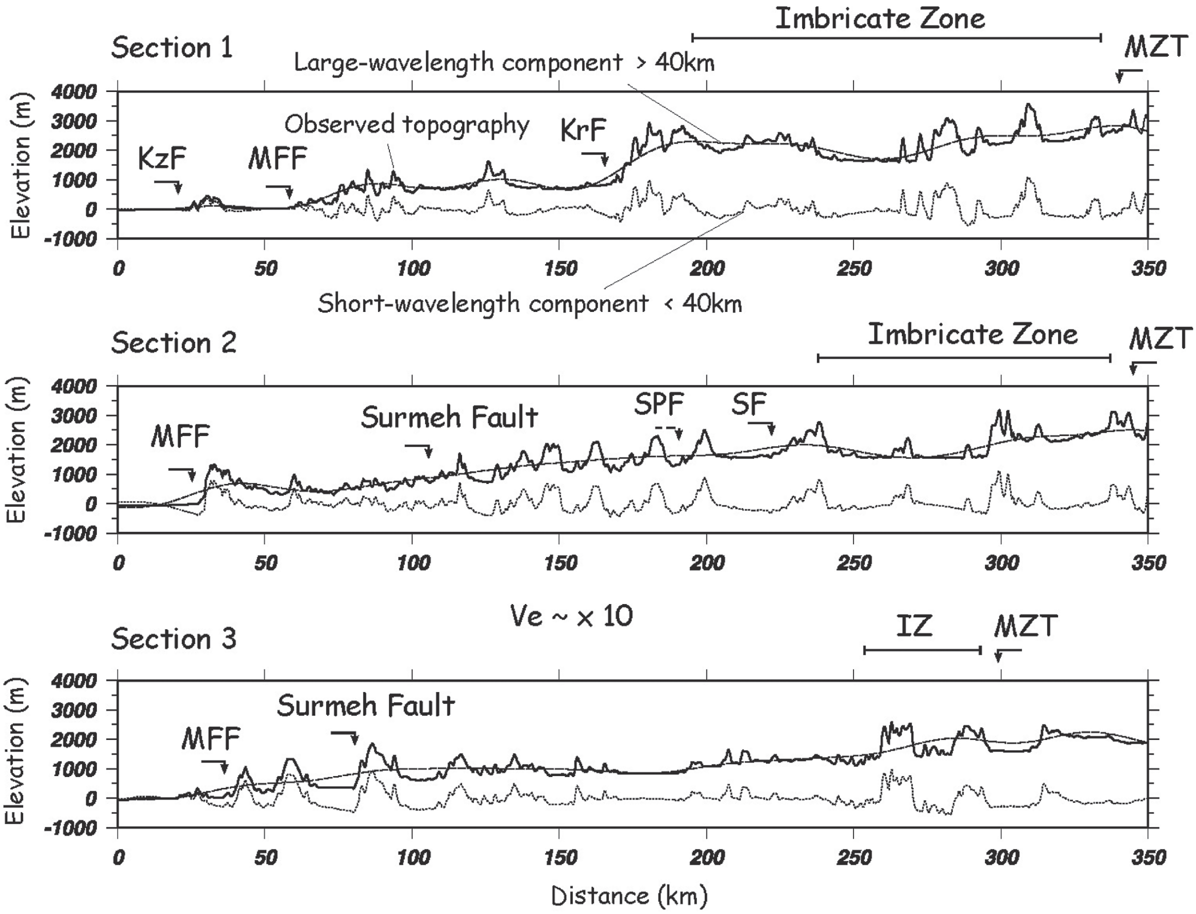

Fig. 15. Wavelength analysis of the topography along transects 1, 2 and 3 (whose location is also presented in Fig. 5). The profiles show the observed topography (*solid lines*) and the filtered topography for both large- and short-wavelength components of the topography (*dashed and dotted lines, respectively*). The main fault zones are the MFF (Mountain Front Fault), SPF (Sabz-Pushan Fault), KzF (Kazerun Fault), KrF (Karebass Fault), SF (Sarvestan fault) and Surmeh (Surmeh Fault). In the northern part of the Fars, the MZT (Main Zagros Thrust) and the Imbricate Zone are also shown

exceed 3–4%. This suggests that even at low depths, viscous-plastic processes were active in cover rocks and has assisted the fold growth.

The reconstructed paleostress orientations from the inversion of calcite twins show a homogeneous mean N020° compression throughout the folded belt and the southern part of the Iranian plateau [Amrouch et al., 2005]. This result is consistent with the compressional stress orientations obtained from the inversion of fault slip data and present-day compression derived from the inversion of focal mechanisms of earthquakes [Lacombe et al., 2006].

Noticeably, all computed stress tensors show a low $\Phi=(\sigma2-\sigma3/\sigma1-\sigma3)$ ratio suggesting that σ2 and σ3 are comparable, accounting for the coeval occurrence of reverse and strike-slip faulting in the cover and the basement. These results suggest that the Hormuz layer, although acting as a major cover-basement décollement and as a mechanical boundary for the upward propagation of most earthquakes, poorly decouples the states of stress within the cover and the basement.

In addition, due to the existence of a constant critical resolved shear stress (CRSS) for twinning, differential stress magnitudes related to a given stress tensor can further be estimated. For a given palaeostress

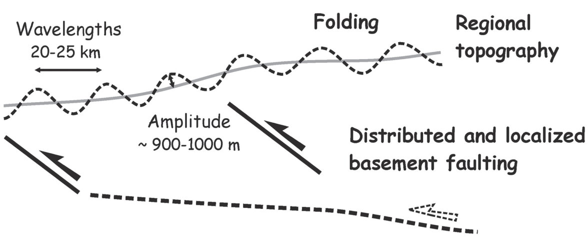

Fig. 16. Schematic representation of the way the different wavelengths of deformation including basement-involved shortening and cover folding interact

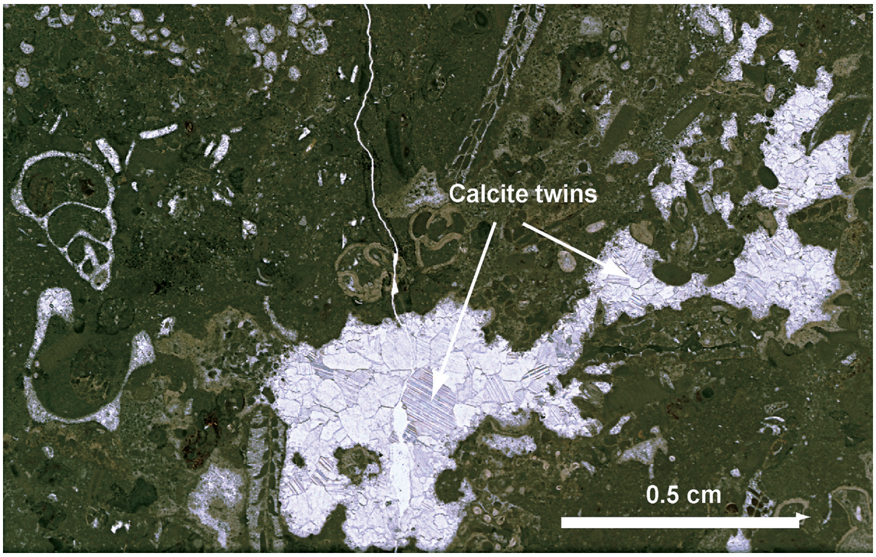

Fig. 17. Photograph illustrating examples of calcite twins formed in vesicles of this shallow-water bioclastic carbonate within the Gashsaran Formation (Meymand fold, northern Central Fars)

orientation, the (σ1-σ3) values correspond to the peak differential stresses attained during the tectonic history of the rock mass.

To a first-order, differential stress values corresponding to the post-folding N020° compression are low and lie within a nearly similar range (45 ± 15 MPa) in the southern Iranian plateau and across the ZFB [Amrouch et al., 2005]. These differential stress values across the ZFB unexpectedly differ from previously reported stress values in fold belts, which are much higher (e.g., 90–150 MPa in the Idaho-Wyoming thrust belt [Craddock and Van der Pluijm, 1999]) and show a strong decay across both the fold belt and the undeformed foreland (e.g., from 100 to 20 MPa in the Sevier-Appalachian forelands: [Van der Pluijm et al. 1997]).

These low and homogeneous stress values highlight major differences in the mechanics of the ZFB compared to other fold belts. The fact that the sedimentary cover sequence is currently aseismic would support that a significant part of the convergence is accommodated by internal ductile mechanisms in the rocks' mass including pression-solution or plastic strain.

The relatively narrow range of variation of differential stress magnitudes across the ZFB agrees with the homogeneously distributed shortening in the folded cover, where no deformation gradient toward the backstop is observed (Fig. 4).

6.3 Mechanical Implications of Cover Buckling

Large-scale critical wedge modelling together with consistency of internal cover plastic (calcite veins) deformation with seismogenic basement stress regime suggest that the cover rocks in the Zagros Folded Belt do not simply behave to first-order as a brittle medium.

Moreover, the sequence of folding has suggested a rapid development of folding coevally across the strike of the belt with no clear evidence of southward propagation. Hereafter, we focus on the possibility that most characteristics of cover folding in the ZFB be explained by buckling.

Several analytical and numerical models have already considered folding in the Zagros Folded Belt as a case example for studying mechanisms of buckling [Biot, 1961; Schmalholz et al., 2002; Turcotte and Schubert, 2002]. The theory of buckling predicts that a single competent layer with random perturbations overlying a weaker matrix will develop into a regular fold train when subjected to layer-parallel shortening [e.g, Biot, 1961; Zhang et al., 1996]. The fold train results from the process of selection and amplification of initial perturbations that is dependent on the competency contrasts between matrix and layer.

Practically, only the perturbations with maximum growth rates will transform into finite folds.

Moreover, the initiation of fold growth is exponential when the dominant wavelength is selected and then gradually slows down. At least three observations may support such development in the Zagros Folded Belt:

1. The rapid growth of folds in probably less than 3 Ma while the collision-related compressive deformation on the Arabian continental margin likely started in Middle Miocene times (ca. 20 Ma);
2. Tolds probably initiated coevally across the ZFB;

3. Progressive onlaps of Bakhtyari conglomerates onto older growth strata suggest a slowing down of fold growth (relatively to the rate of deposition).

The thick Paleozoic and Mesozoic carbonates can be treated as a single competent layer overlying a homogeneous and finite viscous matrix lying in the Cambrian salts. It has been noticed for years that the pure elastic solution for buckling dominant wavelengths given by

$$\lambda_b = 2\pi H \sqrt{E/\sigma}$$

often requires unrealistic high layer-parallel stress σ to fit observed buckling wavelengths. However, it has been proposed that folding wavelengths averaged to values of ~20 km in the ZFB may be roughly approximated by a brittle-elastic solution [Mouthereau et al., 2006]. Indeed, the observed wavelengths can be reproduced assuming a layer-parallel stress that must be at least 300 MPa and a low value of Young's modulus E of 10^9 Pa as suggested by recent mechanical experiments on Miocene carbonates [Amrouch, 2005]. The result is however largely dependent on the effective elastic thickness H we chose for the competent layer. A value of less than 2 km, i.e., representing only a quarter of the value of the unfolded layer, i.e. the thickness of the sedimentary cover, is compatible with fold curvature-1 (> 10^{-5} m) and brittle yielding in a brittle/elastic layer. If this mechanism may account for the failure of the thin-skinned critical wedge model and the sequence of folding, it however fails to reproduce the internal pression-solution processes observed and supported by the poor seismogenic potential of the cover sequence.

On the other hand, a pure viscous solution for buckling dominant wavelengths given by

$$\lambda_b = 2\pi H 6^{-1/3} \sqrt[3]{\eta_l/\eta_m}$$

is limited by viscosity contrasts between layer and matrix of less than two orders of magnitudes [Schmalholz et al., 2002]. The viscosity of the Hormuz evaporites has typical viscosities (Newtonian) of salts between 10^{17} and 10^{18} Pa s. In that case, fold wavelengths may be reproduced using a viscous layer of H=2 km with viscosity η_l of 10^{19} Pa s.

There are several limitations to both models. First they assume infinitesimal deformation which is only applicable at the initial stages of folding. Second, they are small-scale models that neglect the effects of gravity. Finally, they implicitly consider that the weak viscous matrix is infinitely thicker than the competent layer, which is obviously not the case in the Zagros; e.g. Fig. 4 shows average ratios of the matrix thickness to layer thickness between 0.1 (1:8) and 0.3 (2:7) maximum. A better fit of the observed wavelengths of folding in the Zagros has been obtained for a more realistic solution involving buckling of a viscous (non-Newtonian)-elastic layer resting on a homogeneous Newtonian matrix with finite thickness [Schmalholz et al., 2002].

Figure 4 shows that from the Imbricate Zone toward the Surmeh Fault, fold wavelengths progressively decrease from 35 km to 11 km as fold amplitudes increase (e.g., Dalu and Sim anticlines in Fig. 2). Then toward the MFF, fold wavelengths increase again from 11 km close to the Surmeh Fault up to 17 km on average. We suggest that folding might have initially developed with homogeneous and relatively lower amplitude/wavelength ratio. Such wavelengths are currently preserved in the Imbricate Zone or close to the MFF. A possible control by basement-involved deformation cannot be excluded. Then as shortening increased, wavelength of folds reduced, limbs rotated, as exemplified by intraformational unconformities, and fold amplitude increased leading to higher amplitude/wavelength ratios. This is especially the case where the southward propagation is limited by the presence of topographic high like the Surmeh Fault.

Conclusions

The aim of the paper was to discuss which type of mechanical behaviour better explains the development of the Zagros folded belt in terms of cover folding, internal deformation of cover rocks and on the regional scale the crustal rheology that led to the observed regional topography.

The available structural studies combined with seismotectonic constraints demonstrate that the basement is necessarily currently involved in collisional deformation. Additional mechanical constraints derived from a critical wedge modelling of the regional topography confirm this result. The basic assumptions in Coulomb critical wedge models and the present day stress regimes together suggest that the state of stress within the upper crust of the Arabian continental margin has everywhere reached the brittle strength of the crust in agreement with Byerlee's law. However, the lack of seismogenic strain derived from the summation of seismic tensors [Jackson et al., 1995] suggests that aseismic deformation is likely to occur in the (lower ?) crust.

In agreement with the failure of a thin-skinned critical wedge model for the Fars, the distribution of deformation in the cover rocks does not display a gradient of deformation increasing rearward (i.e., toward the MZT) as it is usually observed for typical thin-skinned thrust wedges.

The thickness distribution of the Mishan Formation suggests that the Arabian continental margin was inverted as early as the Middle Miocene in response to continent-continent collision. Margin inversion occurred by the reactivation of NW-SE-trending Tethyan normal faults (e.g., Surmeh Fault, Mountain Front Fault) and Panafrican inherited N-S fault trend (Karebass, Sabz-Pushan, Sarvestan transcurrent faults). During this episode, the sedimentary cover suffered little shortening near active basement faults and deformation was localized along the main basement faults, i.e., the Surmeh Fault and the MFF. This episode is probably a consequence of the intraplate stress build up in the margin following the initiation of the collision.

By the Pliocene-Pleistocene period, cover folding developed rapidly in a few million years all over the ZFB in agreement with the field observations of growth strata associated with folds uplift. At this point, the foreland basin transformed into an orogenic belt controlled by the propagation of a brittle upper crustal wedge. Reverse movements along already inverted basement structures (MFF and Surmeh Fault) increased and faulting was generalized within the upper brittle crust, leading to the current seismic activity in the ZFB. At the same time, the growth of folds rapidly diminished as suggested by the observations that youngest syn-orogenic strata (Bakhtyari Fm) often onlap older synfolding strata (upper Agha Jari Fm).

Observations in the field of the internal deformation of rocks reveal that the rheology of the sedimentary cover during folding was dominated by viscous-plastic and local brittle behaviours. Numerous characteristics of cover folding suggest that folds developed mainly as buckle folds. A mechanical model involving a viscous (non-Newtonian)-elastic layer representing the thick cover (~10 km) resting on a homogeneous Newtonian matrix represented by the Hormuz salt satisfactory reproduces the observed distribution of folds widths.

We conclude that the distributed thick-skinned deformation that followed the initial margin inversion occurred coevally with the main phase of cover folding. The way they deform however is different; the basement is pre-fractured so it shortens preferentially by faulting. In contrast, the folding of the thick sedimentary cover developed by buckling over an incompetent layer of salt with the assistance of plastic-viscous processes.

Acknowledgments

This work has been supported by the Middle East Basin Evolution (MEBE) program.

The authors thank the Geological Survey of Iran for its support for fieldwork and especially A. Saidi, P. Navabpour. We are indebted to John Cosgrove, Stephane Homke and Jaume Vergès for their thoughtful reviews of the manuscript.

References

Agard, P., J. Omrani, L. Jolivet, and F. Mouthereau, Convergence history across Zagros (Iran): constraints from collisional and earlier deformation, Intern. Journ. of Earth Sciences, doi:10.1007/s00531-005-0481-4, 2005.

Ahmadhadi, F., O. Lacombe, and J.-M. Daniel, Early reactivation of basement faults in Central Zagros (SW Iran): evidence from pre-folding fracture patterns in Asmari Formation and Lower Tertiary paleogeography, this issue.

Amrouch, K., Quantification des orientations et des magnitudes les paléocontraintes tertiaires dans la chaîne plissée du Zagros par l'analyse des macles de la calcite, Master thesis, Université P. et M. Curie (Paris 6), Paris, France, 2005.

Amrouch, K., O. Lacombe, F. Mouthereau, and L. Dissez, Quantification of orientations and magnitudes of the late Cenozoic paleostresses in the Zagros folded belt from calcite twin analysis, in Thust Belts and Foreland Basins, International Meeting, Rueil-Malmaison, 31–35, 2005.

Bahroudi, A., and H.A. Koyi, Effect of spatial distribution of Hormuz salt on deformation style in the Zagros fold and thrust belt: an analogue modelling approach, Journ. of Geolog. Soc. of London, 160, 1–15, 2003.

Baker, C., J.A. Jackson, and K. Priestley, Earthquakes on the Kazerun Line in the Zagros mountains of Iran: Strike-slip faulting within a fold-and-thrust belt, Geophys. Journ. Intern., 115, 41 – 61, 1993.

Berberian, M., Master "blind" thrust faults hidden under the Zagros folds: active basement tectonics and surface tectonics surface morphotectonics, Tectonophysics, 241, 193–224, 1995.

Berberian, M., and G.C.P. King, Towards a paleogeography and tectonic evolution of Iran, Canadian Journal of Earth Sciences = Journal Canadien des Sciences de la Terre, 18, 210–265, 1981.

Biot, M.A., Theory of folding of stratified viscoelastic media and its implications in tectonics and orogenesis, Geological Society of America Bulletin, 72, 1595–1620, 1961.

Blanc, E.J.-P., M.B. Allen, S. Inger, and H. Hassani, Structural styles in the Zagros simple folded zone, Iran, Journal of the Geological Society of London, 160, 401–412, 2003.

Craddock, J.P., and B.A. van der Pluijm, Sevier-Laramide deformation of the continental interior from calcite twinning analysis, west-central North America, Tectonophysics, 305, 275–286, 1999.

Costa, E., and B.C. Vendeville, Experimental insights on the geometry and kinematics of fold-and-thrust belts above weak, viscous evaporitic décollement, Journ. of Struct. Geol., 24, 1729–1739, 2002.

Davis, D.M., and T. Engelder Role of Salt in Fold-and-Thrust Belts, Tectonophysics, 119,6788, 1985.

De Mets, C., R.G. Gordon, D.F. Argus, and S. Stein, Effects of recent revision to the geomagnetic reversal time scale on estimates of current plate motions, Geophysical Research Letters, 2191–2194, 1994.

Elmore, R.D., and W.R. Farrand, Asphalt-bearing sediment in synorogenic Miocene-Pliocene molasse, Zagros Mountains, Iran, American Association of Petroleum Geologists Bulletin, 65, 1160–1165, 1981.

Falcon, N.L., Major earth-flexuring in the Zagros Mountains of south-west Iran, Quarterly Journ. of the Geol. Soc. of London, 177, 367–376, 1961.

Hatzfeld, D., M. Tatar, K. Priestley, and M. Ghafori-Ashtiany, Seismological constraints on the crustal structure beneath the Zagros Mountain Belt (Iran), Geophys. Journ.l Intern., 403–410, 2003.

Hessami, K., H.A. Koyi, C.J. Talbot, H. Tabasi, and E. Shabanian, Progressive unconformities within an evolving foreland fold-thrust belt, Zagros Mountains, Journ. of the Geol; Soc., 158, 969–981, 2001.

Homke, S., J. Verges, G. Garces, H. Emamia, and R. Karpuzc, Magnetostratigraphy of Miocene–Pliocene Zagros foreland deposits in the front of the Push-e Kush Arc (Lurestan Province, Iran), Earth and Planetary Science Letters, 225, 397–410, 2004.

Jackson, J., J. Haines, and W. Holt, The accommodation of Arabia-Eurasia plate convergence in Iran, Journ. of Geophys. Research, 100, 15,205–15,219, 1995.

Jackson, J.A., Reactivation of basement faults and crustal shortening in orogenic belts,Nature, 283, 343–346, 1980.

Jackson, M.P.A., R.R. Cornelius, C.H. Craig, A. Gansser, J. Stöcklin, and C.J. Talbot, Salt diapirs of the Great Kavir, central Iran, in Geological Society of America Memoir, vol. 177, pp. 139, The Geological Society of America, Boulder, 1990.

Koop, W., and R. Stoneley, Subsidence history of the middle East Zagros basin, Permian to Recent, Philosophical Transation of the Royal Society of London, 305, 149–168, 1982.

Lacombe, O., F. Mouthereau, S. Kargar, and B. Meyer, Late Cenozoic and modern stress fields in the western Fars (Iran): Implications for the tectonic and kinematic evolution of central Zagros, Tectonics, 25, doi:10.1029/2005TC001831, 2006, 2006.

Maggi, A., J.A. Jackson, K. Priestley, and C. Baker, A re-assessment of focal depth distributions in southern Iran, the Tien Shan and northern India: do earthquakes really occur in the continental mantle ?, Geophysical Journal International, 143, 629–661, 2000.

McQuarrie, N., Crustal scale geometry of the Zagros fold-thrust belt, Iran, Journ. of Struct. Geol., 519–535, 2004.

McQuarrie, N., J.M. Stock, C. Verdel, and B.P. Wernicke, Cenozoic evolution of Neotethys and implications for the causes of plate motions, Geophysical Research Letters, 30, doi:10.1029/2003GL017992, 2003.

Molinaro, M., P. Leturmy, J.-C. Guezou, D. Frizon de Lamotte, and S.A. Eshraghi, The structure and kinematics of the south-eastern Zagros fold-thrust belt; Iran: from thin-skinned to thick-skinned tectonics, Tectonics, 24, doi:10.1029/2004TC001633, 2005a.

Molinaro, M., H. Zeyen, and X. Laurencin, Lithospheric structure underneath the SE Zagros Mountains, Iran: recent slab break-off?, Terra Nova, 25, 1–6, 2005b.

Molnar, P., and P. England, Late Cenozoic uplift of mountain ranges and global climate change: chicken or egg ?, Nature, 346, 29–34, 1990.

Motiei, H., Geology of Iran : Stratigraphy of Zagros, 536 pp., Geological Survey of Iran, 1993.

Mouthereau, F., O. Lacombe, and B. Meyer, The Zagros Folded Belt (Fars, Iran): Constraints from Topography and Critical Wedge Modelling, Geophys. Journ. Intern., 165, 336–356, 2006.

Ni, J., and M. Barazangi, Seismotectonics of the Zagros continental collision zone and a comparison with the Himilayas, Journal of Geophysical Research, 91, 8205–8218, 1986.

National Iranian Oil Company, N.I.O.C., Geological map of Iran, sheet 5, South-central Iran, Tehran, 1977.

Oveisi, B., J. Lavé, and P. Van der Beek, Active folding and deformation rate at the central Zagros front (Iran), this issue.

Schmalholz, S.M., Y. Podladchikov, and J.P. Burg, Control of folding by gravity and matrix thickness: implications for large-scale folding, Journ. of Geophys. Research, 107, 10.1029/2001JB000355, 2002.

Schuster, F., and U. Wielandt, Oligocene and Early Miocene coral faunas from Iran: palaeoecology and palaeobiogeography, Intern. Journ.l of Earth Sciences, 88, 571–581, 1999.

Sepher, M., and J.W. Cosgrove, Structural framework of the Zagros Fold-Thrust Belt, Iran, Marine and Petroleum Geology, 21, 829–843, 2004.

Sherkati, S., and J. Letouzey, Variation of structural style and basin evolution in the central Zagros (Izeh zone and Dezful Embayment), Iran, Marine and Petroleum Geology, 21, 535–554, 2004.

Snyder, D.B., and M. Barazangi, Deep crustal structure and flexure of the Arabian plate beneath the Zagros collisional mountain belt as inferred from gravity observations, Tectonics, 5, 361–373, 1986.

Stocklin, J., Structural history and tectonics of Iran; a review, American Association of Petroleum Geologists Bulletin, 52, 1229–1258, 1968.

Stoneley, R., The Arabian continental margin in Iran during the Late Cretaceous, in The Geology and Tectonics of the Oman Region, edited by A.H.F. Robertson, M.P. Searle and A.C. Ries, pp. 787–795, 1990.

Talbot, C.J., and M. Alavi, The past of a future syntaxis across the Zagros, in Alsop, in Salt Tectonics, vol. 100, edited by G.I. Alsop, D.J. Blundell. and I. Davison, pp. 89–109, Geological Society of America Special Paper, 1996.

Talebian, M., and J.A. Jackson, A reappraisal of earthquake focal mechanisms and active shortening in the Zagros mountains of Iran, Geophys. Journ. Intern., 156, 506–526, 2004.

Tatar, M., D. Hatzfeld, and M. Ghafori-Ashtiany, Tectonics of the Central Zagros (Iran) deduced from microearthquakes seismicity, Geophysical Journal International, 255266, 2004.

Turcotte, D.L., and G. Schubert, Geodynamics: Applications of Continuum Mechanics to Geological Problems, Cambridge University Press, 2002.

Van der Pluijm, B.A., J.P. Craddock, B.R. Graham, and J.H. Harris, Paleostress in Cratonic North America: Implications for Deformation of Continental Interiors, Science, 277, 794–796, 1997.

Vernant, P., F. Nilforoushan, D. Hatzfeld, M.R. Abbassi, C. Vigny, F. Masson, H. Nankali, J. Martinod, A. Ashtiani, R. Bayer, F. Tavakoli, and J. Chéry, Present-day crustal deformation and plate kinematics in the Middle East constrained by GPS measurements in Iran and northern Oman, Geophysical Journal International, 157, 381–398, 2004.

Walpersdorf, A., D. Hatzfeld, H. Nankali, F. Tavakoli, F. Nilforoushan, M. Tatar, P. Vernant, J. Chéry, and F. Masson, Difference in the GPS deformation pattern of North and Central Zagros (Iran), Geophysical Journ. Intern., in press.

Weijermars, R., J.A. Jackson, and B. Vendeville, Rheological and tectonic modeling of salt provinces, Tectonophysics, 217, 143–174, 1993.

Williams, C.A., C. Connors, F.A. Dahlen, E.J. Price, and J. Suppe, Effect of the brittle-ductile transition on the topography of compressive mountain belts on Earth and Venus, Journal of Geophysical Research, 99, 19,947–19,974, 1994.

Zhang, Y., B.E. Hobbs, A. Ord, and H.B. Mühlhaus, Computer simulation of single-layer buckling, Journal of Structural Geology, 18, 643–655, 1996.

Ziegler, M.A., Late Permian to Holocene Paleofacies Evolution of the Arabian Plate and its Hydrocarbon Occurrences, GeoArabia, 6, 445–503, 2001.